

Calorimetric analysis of the multiple melting behavior of melt-crystallized poly(L-lactic acid) with a low optical purity

Ping Song · Guangyi Chen · Zhiyong Wei ·
Wanxi Zhang · Jicai Liang

Received: 19 August 2011 / Accepted: 18 May 2012 / Published online: 3 July 2012
© Akadémiai Kiadó, Budapest, Hungary 2012

Abstract The polymorphous crystallization and multiple melting behavior of poly(L-lactic acid) (PLLA) with an optical purity of 92 % were investigated after isothermally crystallized from the melt state by wide-angle X-ray diffraction and differential scanning calorimetry. Owing to the low optical purity, it was found that the disordered (α') and ordered (α) crystalline phases of PLLA were formed in the samples crystallized at lower (<95 °C) and higher (≥ 95 °C) temperatures, respectively. The melting behavior of PLLA is different in three regions of crystallization temperature (T_c) divided into Region I ($T_c < 95$ °C), Region II (95 °C $\leq T_c < 120$ °C), and Region III ($T_c \geq 120$ °C). In Region I, an exothermic peak was observed between the low-temperature and high-temperature endothermic peaks, which results from the solid–solid phase transition of α' -form crystal to α one. In Region II, the double-melting peaks can be mainly ascribed to the melting–recrystallization–remelting of less stable α crystals. In Region III, the single endotherm shows that the α crystals formed at higher temperatures are stable enough and melt directly without the recrystallization process during heating.

Keywords Multiple melting behavior · Poly(L-lactic acid) · Polymorphous crystallization · Phase transition

Introduction

Poly(L-lactic acid) (PLLA) has attracted much attention in recent years particularly from the environmental and ecological perspectives due to the compostability and producibility from renewable resources [1]. Because of its bioresorbable and biocompatible features, PLLA is expected to be used for medical applications, such as surgical sutures, bone fixation, and controlled drug release matrices [2]. Furthermore, concerning its favorable biodegradability, renewability, good mechanical properties, and versatile fabrication processes, PLLA has excellent potential for substitution of petroleum-based polymers [3].

PLLA displays crystalline polymorphism and crystallizes in α -, β -, or γ -form depending on the crystallization conditions [4–11]. The most common α -form of PLLA grows upon melt or cold-crystallization, as well as from solution under normal conditions. The α -form has a 10_3 helical conformation where two antiparallel left-handed chains pack in an orthorhombic or pseudo-orthorhombic unit cell [4–7]. The β -form was prepared by stretching the α -form at high drawing ratio and high temperature [8–10]. The γ -form, developed via epitaxial crystallization on hexamethylbenzene substrate, was proposed by Cartier et al. [11]. Recently, Zhang et al. [12, 13] reported that a disordered form of α' crystal, i.e., α' modification, was likely to be produced in PLLA crystallized at temperature below 120 °C. Compared to α -form, the α' modification is conformation-disordered and has a loose chain-packing manner. The WAXD patterns of the α' and α forms of PLLA are very similar with small differences seen in the appearance of a weak reflection at $2\theta \approx 24.6^\circ$ only in the α' modification, and in the shift to higher 2θ of the two strongest (110)/(200) and (203) reflections, indicating that the α' -form has slightly larger lattice spacing than α counterpart [14, 15].

P. Song · G. Chen · Z. Wei (✉) · W. Zhang · J. Liang
School of Automotive Engineering,
Dalian University of Technology,
Dalian 116024, China
e-mail: zywei@dlut.edu.cn

In recent years, the crystallization process of PLLA has received considerable research interest [16–19]. It has been found that the crystallization behavior of PLLA is peculiar in the range 100–120 °C, showing that the crystallization kinetics is discontinuous in this temperature range by a clear deviation from the usual bell-shaped curve of T_c dependence of crystallization half-time or spherulite growth rate [20–22]. This discontinuity has been correlated to the regime transition from II to III, while Lorenzo [20, 21] argued that it should be ascribed to a sudden acceleration in spherulite growth. Moreover, Zhang et al. [12, 13] proposed that the most possible explanation might be the difference in the crystal modifications. Despite extensive studies of PLLA, the crystallization and melting behavior are still not completely understood. Especially, the melting of semicrystalline thermoplastic is a very complex process, which is influenced significantly by the crystallization conditions.

Double or multiple melting behavior has been observed in many semicrystalline polymers such as polypropylene (PP) [23, 24], polystyrene (PS) [25], poly(ether ether ketone) (PEEK) [26–28], poly(ethylene terephthalate) (PET) [29, 30], poly(butylene-2,6-naphthalate) (PBN) [31], poly(trimethylene terephthalate) (PTT) [32], and some biodegradable aliphatic polyesters, e.g., poly(butylene succinate) and copolymers [33–35]. It is an important research subject in the field of polymer science to gain a basic understanding of the structural evolution related to thermal history (i.e., crystallization conditions) and to provide a deep insight into the crystallization and melting processes of semicrystalline polymers. As summarized in the literature [25, 36, 37], possible origins of the complex melting phenomenon are as follows: (1) the presence of more than one crystal forms (polymorphism), (2) the presence of different morphologies (such as lamellar thickness, distribution, perfection, or stability), (3) melting, recrystallization, and remelting processes during heating, (4) physical aging and/or relaxation of the rigid amorphous fraction, (5) different molecular weight species, and so on.

Likewise, PLLA also shows the multiple melting peaks in the DSC heating scan. According to the conventional and temperature-modulated DSC analysis, this behavior was proposed to originate from the melt–recrystallization mechanism by several research groups [38–44]. Besides, another possible interpretation was due to the phase transition from α' -form crystal to α one and the melting of the as-transformed α crystals. Obviously, there exist more or less divergences among these different melting mechanisms, and up to now, no consensus has been reached as for the exact origin of multiple melting behavior of PLLA [45–49]. Therefore, a further investigation of the melting behavior of PLLA is needed to deeply understand the origin of this phenomenon.

It is well known that the optical purity (OP) of PLLA strongly affects its crystallization kinetics and melting behavior [50–54]. The crystallization rate, crystallinity, and melting point decrease with a reduction of optical purity [52, 53], and PLLA loses crystallizability when the level of OP is smaller than 76 % [54]. Usually, PLA used for large-scale applications is the random copolymers containing predominantly L-isomer and small amounts of D-isomer [1, 49]. However, most of the studies are focused on optically pure PLLA, i.e., $OP \geq 98\%$. In this work, we intend to investigate the melting behavior of PLLA with a low optical purity of 92 % under various crystallization and heating processes and to improve the understanding of the mechanism of multiple melting peaks. The observed peculiarity is discussed in the context of models considering both the solid state transition of the two different crystalline phases and the melt–recrystallization process as a function of crystallization temperature.

Experimental

Materials

An injection grade poly(L-lactic acid) (PLLA, Biopla 305D) resin used in this study with a density of 1.25 g cm^{-3} and melt flow index of $10\text{--}13 \text{ g } 10 \text{ min}^{-1}$ (2.16 kg, 190 °C) was purchased from Biopla Products Factory, China. The number-averaged and weight-averaged molecular weights were determined by gel permeation chromatography (GPC) as 71 000 and 118 000 Da, respectively. The rotatory power ($[\alpha_L^{25}]$) was measured in chloroform at a concentration of 1 g dL^{-1} and at 25 °C using a Jasco P-1010 polarimeter at a wavelength of 589 nm. The optical purity (OP) was calculated by the following equation:

$$OP (\%) = \frac{[\alpha_L^{25}]}{[\alpha_L^{25}]_0} \times 100 \quad (1)$$

where $[\alpha_L^{25}]_0$ is the rotatory power of the optically pure PLLA and its value is taken as -156° [51]. $[\alpha_L^{25}]$ of the analyzed PLLA was determined to be -144° , thus a value of 92 % was obtained for OP. Before any characterization, the PLLA samples were dried at 60 °C overnight in a vacuum oven to prevent hydrolysis and thermal degradation.

Differential scanning calorimetry (DSC)

Isothermal crystallization was performed in a DSC1 (Mettler-Toledo, Switzerland) differential scanning calorimeter. The instrument was calibrated using high purity indium and zinc standards. Each sample (ca. 5 mg) was

initially melted at 185 °C for 5 min to erase the previous thermal history and then cooled rapidly to the selected isothermal crystallization temperature (T_c). To prevent further crystallization occurring on cooling, the samples were heated at 10 °C min⁻¹ immediately from T_c to 185 °C after the completion of isothermal crystallization. For studying the effect of heating rate on the melting behavior, the samples were scanned from 5 to 20 °C min⁻¹. All the measurements were repeated three times to improve accuracy [55].

Wide-angle X-ray diffraction (WAXD)

PLLA sheets (ca. 1-mm thickness) were prepared by melting the samples on a hot plate (ca. 180 °C) and compressed between two metallic disks. Then, they were quickly transferred to an oven and annealed at the preset temperature. WAXD analysis was performed on a D/max-Ultima + X-ray diffractometer (Rigaku, Japan) with Ni-filtered Cu K α radiation ($\lambda = 0.15418$ nm) at room temperature (ca. 20 °C). The operating target voltage was 40 kV and the tube current was 100 mA. Scans were made from 10 to 30° at a rate of 1.2° min⁻¹.

Results and discussion

Effect of crystallization temperature

Crystallization temperature has a significant effect on the melting behavior of semicrystalline polymers. Figure 1 shows the DSC curves of PLLA samples isothermally melt-crystallized at different temperatures (T_c s). Three kinds of different melting behaviors could be identified with increasing T_c from 80 to 130 °C. When $T_c < 95$ °C, the DSC curve is characterized by a small exothermic peak (denoted as T_{exo}) between the low-temperature endothermic peak I (T_{m1}) and the high-temperature endothermic peak II (T_{m2}). Peak I is very weak and peak II is more prominent than peak I. When 95 °C $\leq T_c < 120$ °C, T_{exo} already disappears, peak I moves to higher temperatures and its magnitude relative to peak II increases with increasing T_c . Meanwhile, the location of peak II remains almost unaltered, but it eventually vanishes and merges with peak I. When $T_c \geq 120$ °C, only a single endothermic peak is observed and it moves to higher temperatures further with increasing T_c . These distinct melting behaviors are analogous with some earlier reports for melt-crystallized PLLA with a slight difference in temperature range [41–45]. Since the melting behavior is greatly dependent on the crystallization behavior, the effect of T_c on polymorphous crystallization of PLLA will be further discussed in the following section.

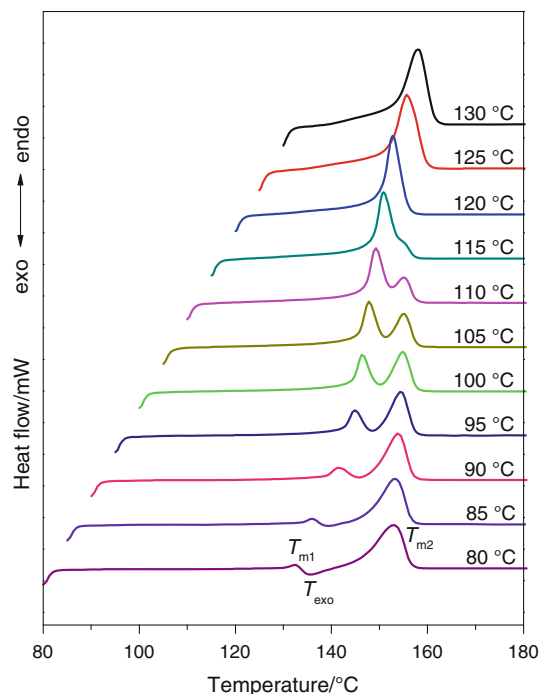
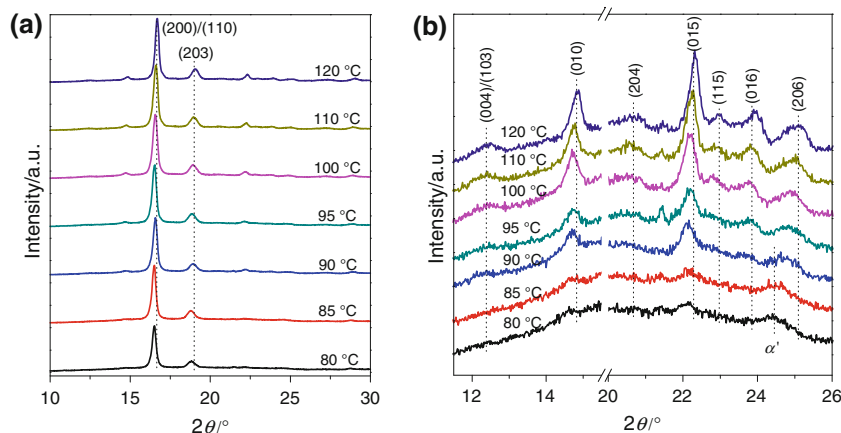


Fig. 1 DSC heating scans obtained at 10 °C min⁻¹ of isothermally melt-crystallized PLLA at indicated temperatures

Crystal form of samples crystallized at T_c s

The WAXD technique was used to examine the polymorphous behavior of samples because the α -form crystal of PLLA exhibits more subtle WAXD patterns than the disordered one (α'). Figure 2 shows the diffractive patterns and the corresponding enlarged patterns of samples after annealed at different T_c s. The assignment of the observed reflections is based on the crystalline structure reported for the α -form crystal of PLLA [5]. It is clear that with increasing T_c from 80 to 120 °C, two strongest reflections of (200)/(110) and (203) planes shift to higher 2θ , the intensities of (010) and (015) reflections increase, and some small diffraction peaks assigned to the reflections of (004)/(103), (204), and (115) emerge at $2\theta = 12.3$, 20.5, and 23.0°, respectively. In addition, two diffraction peaks of the α -form, attributed to (016) at 23.8° and (206) at 25.1°, are present instead of the characteristic diffraction of the α' crystal of PLLA at 24.5° when T_c is higher than 95 °C. These results suggest that the critical temperature for polymorphous crystallization of the PLLA used in this study is ~ 95 °C, i.e., α' and α crystals are mainly formed at $T_c < 95$ °C and $T_c \geq 95$ °C, respectively. In view of optically pure PLLA, it was found to crystallize as the α -form when crystallization took place at temperatures higher than 120 °C, while the α' modification developed at T_c s below 120 °C [12, 16]. The temperature range, where each of the two polymorphs prevails for the analyzed

Fig. 2 WAXD patterns (a) and expanded WAXD patterns (b) of melt-crystallized PLLA at different temperatures



PLLA, is substantially lower than the one reported by the literature [14, 15, 45, 49, 55–57].

From Fig. 1, it can be seen that the melting temperature range of the PLLA samples is between 140 and 160 °C, which is far below the range of optically pure PLLA in 160–180 °C. For random copolymers, the melting-point depression as a function of composition can be described by Flory's equation:

$$\frac{1}{T_m^0} - \frac{1}{T_m^0} = -\frac{R}{\Delta H_f^0} \ln(1-p) \quad (2)$$

or

$$T_m^0 - T_m^0 = \frac{-RT_m^0 T_m^0}{\Delta H_f^0} \ln(1-p) \cong \frac{R(T_m^0)^2}{\Delta H_f^0} p \quad (3)$$

where T_m^0 and T_m^0 are the equilibrium melting points of the copolymer and homopolymer, respectively. ΔH_f^0 is the enthalpy of fusion, R is the gas constant, and p is the probability that the next residue in a crystallizing chain will be a defect [52]. In the case of poly(L-lactide-co-D-lactide) or poly(L-lactide-co-meso-lactide), the value of p increases with decreasing OP because the D-isomer units are excluded from PLLA crystalline lamellae as defects [58, 59]. According to Eq. 3, it can be concluded that the equilibrium melting point of PLLA is depressed as a result of the low optical purity. Moreover, the crystallization rate of PLLA also decreases with a decrease of optical purity [52–54]. It was reported that both the lowered equilibrium melting point and decreased crystallization rate could lead to the reduction of critical temperature for generating the PLLA α' - and α -form crystals [60]. A previous study has evidenced that α crystals rather than α' ones were induced in the PLLA with an optical purity of 88 % by compressed CO₂ at temperatures as low as 65 °C [50]. In contrast, the molecular weight was found to hardly affect the temperature range for polymorphism of PLLA [14]. Consequently, it is reasonable to consider that the low optical purity of the

used PLLA accounts for the generation of the α -form crystals at relatively lower temperatures, as revealed in Fig. 2.

Region

The data of the melting points of PLLA isothermally melt-crystallized at different T_c s were obtained by heating at a rate of 10 °C min⁻¹, and T_c dependence of T_m is shown in Fig. 3. The solid lines in the figure represent the linear fitting curves of these melting temperatures. It is seen that dT_{m1}/dT_c discretely changes at ~ 95 °C, indicating that two different crystalline phases develop below or above this critical temperature, which is in agreement with the abovementioned WAXD results. Noting that double-melting peaks turn into single endotherm at ~ 120 °C, thus, T_c can be divided into three regions: Region I ($T_c < 95$ °C), Region II (95 °C $\leq T_c < 120$ °C), and Region III ($T_c \geq 120$ °C). On the basis of DSC and WAXD measurements, the characteristics of the melting behavior in these three temperature regions are as follows:

Region I ($T_c < 95$ °C)

Endothermic peak I (T_{m1}) originates from the partial melting of α' -form crystals developed upon the isothermal crystallization, whereas endothermic peak II (T_{m2}) corresponds to the melting of α crystals produced in the phase transition. Because of the low and high thermal stability of the initial α' crystals and transformed α ones, T_{m1} increases sharply with T_c , whereas T_{m2} varies slightly as shown in Fig. 3. The small exothermic peak situated between the two melting endotherms has been confirmed to arise from the disorder-to-order (α' - α) phase transition in which the chain packing of the crystalline lattice becomes more compacted and the chain conformation rearranges slightly [12, 14].

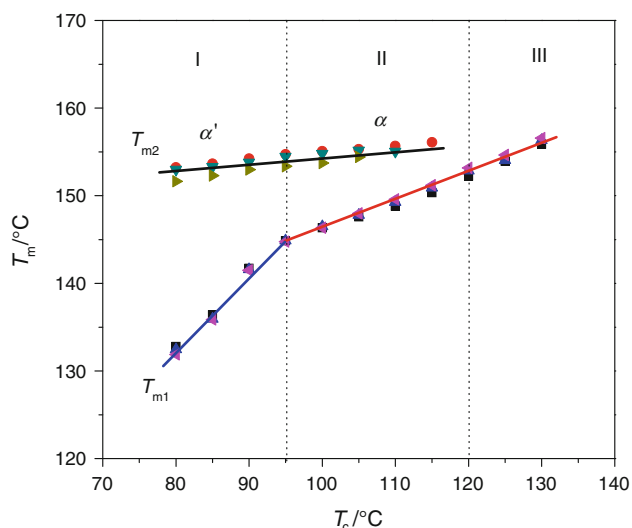


Fig. 3 Dependence of melting point (T_m) on crystallization temperature (T_c)

As distinguished from the usual melt–recrystallization process, the transformation from α' to α crystal is via a solid–solid phase transition mechanism in light of the observations that (1) no decrease in the wide-angle and small-angle X-ray scattering intensities presents on the occasion of the phase transition [16], (2) the X-ray fiber pattern keeps the high degree of chain orientation during the transition [57], and (3) the infrared spectral features in the 1,260–1,160 cm^{-1} range of the α crystal produced in the phase transition process are different from those of the normal α -form developed by the melt-crystallization at the same temperature [61]. It should be pointed out that only partial α' -form crystals transform into the α ones, and some amounts of the α' -form crystals melt directly during the heating scans, which give rise to the small exothermic peak and low-temperature endothermic peak in the DSC curves. Therefore, the multiple melting behavior of the PLLA samples crystallized in Region I can be attributed to the direct melting of partial α' crystals, α' -to- α crystalline phase transition, and the melting of the as-transformed α crystals.

Region II ($95\text{ }^\circ\text{C} \leq T_c < 120\text{ }^\circ\text{C}$)

The samples crystallized at temperatures in this region mainly consist of the α crystalline phase and demonstrate the typical double-melting behavior. T_{m1} increases gradually with increasing T_c , whereas T_{m2} keeps almost constant at $155.0 \pm 0.5\text{ }^\circ\text{C}$. Owing to the lack of α' modification, the two endotherms of the samples crystallized in this temperature region can be explained well by the melt–recrystallization mechanism. The imperfect or less stable α crystals generated at T_c go through the continuous melting/structural reorganization/crystal perfection processes

upon heating. The lower temperature peak I is attributed to the melting of primary α crystals, and the higher temperature peak II corresponds to the melting of the recrystallized α crystals [14, 38, 39].

Region III ($T_c \geq 120\text{ }^\circ\text{C}$)

The melting endotherm of PLLA crystallized in this region displays as a single peak corresponding to the melting of the α crystals formed in the isothermal crystallization process. T_{m1} increases almost linearly with T_c as shown in Fig. 3, which is consistent with the Hoffman–Weeks theory [62]. It is well known that the undercooling, i.e., $T_m^0 - T_c$, plays an important role for semicrystalline polymers to undergo recrystallization during heating. When they crystallize at larger undercooling, the formed crystals are less perfect and are therefore relatively prone to reorganize into a crystal population with a higher thermodynamic stability during heating. However, at smaller undercooling, the crystals are much more perfect and less susceptible to reorganization. The single melting peak of PLLA crystallized in Region III indicates that the as-produced α crystals are stable enough and melt directly without the recrystallization process at the small undercooling.

Effect of heating rate

Measurement of the heating rate effects on the melting behavior is a common method to test the existence of melt–recrystallization phenomenon since it requires suitable time for the recrystallization process and DSC endotherms change their shapes with the heating rate. According to the melt–recrystallization–remelting model [26, 27], the small and imperfect crystals will change successively into more stable crystals with the increase in temperature. At higher heating rates, the sample passes through the recrystallization region so rapidly that there is insufficient time for the melted materials to reorganize into new crystals. Hence, the reorganization process is largely inhibited. The amount and perfection of the recrystallized crystals decrease with increasing the heating rate, which contributes to the decrease of the high-temperature endothermic peak in magnitude. In general, increasing heating rate allows less time for the crystals to reorganize and the remelting occurs at a lower temperature range. Ideally, the melting of reorganized crystals should completely vanish over certain heating rate when the recrystallization is totally inhibited.

The heating rate effect was studied for the PLLA samples melt-crystallized at 90 and 110 $^\circ\text{C}$ after the completion of crystallization. As shown in Fig. 4, the heating rate effect is evident in samples crystallized at 110 $^\circ\text{C}$. At heating rates lower than $10\text{ }^\circ\text{C min}^{-1}$, distinctive double-melting

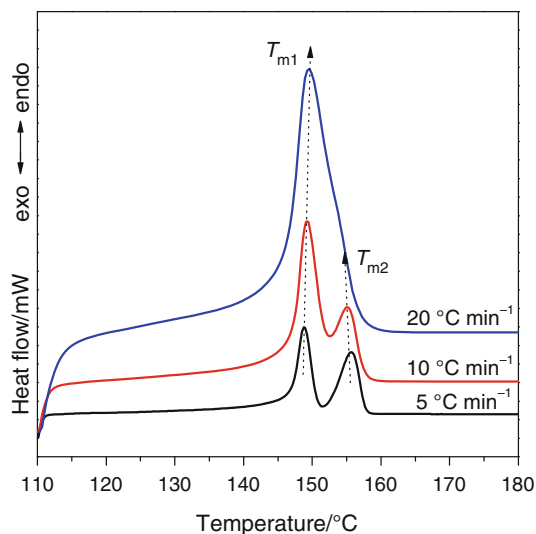


Fig. 4 DSC heating scans of PLLA recorded by different heating rates from 5 to 20 °C min⁻¹ after melt-crystallized at 110 °C

phenomena are observed. It is clear that the relative intensity of peak I to peak II increases with increasing heating rate. Eventually, when the heating rate exceeds 10 °C min⁻¹ up to 20 °C min⁻¹, only one melting peak is discernible, and the peak I temperature gradually increases as superheating becomes more severe with increasing heating rate. As anticipated, the continued increase of heating rate ultimately hinders the recrystallization leading to the single melting peak. These results confirm that the double-melting behavior of samples crystallized in Region II is mainly derived from the melting–recrystallization–remelting processes upon heating.

However, for the PLLA samples crystallized at 90 °C, the position of melting peak I locates constant at 141.5 ± 0.1 °C, independent of the heating rate, and the

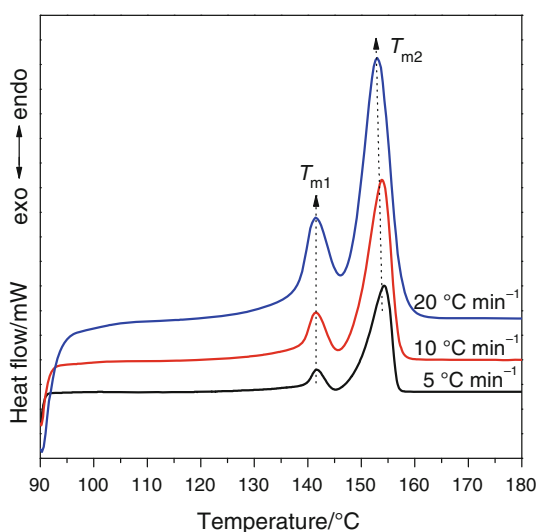


Fig. 5 DSC heating scans of PLLA recorded by different heating rates from 5 to 20 °C min⁻¹ after melt-crystallized at 90 °C

intensity of peak II does not weaken with increasing heating rate from 5 to 20 °C min⁻¹ as shown in Fig. 5. The double-melting peaks of samples crystallized at 90 °C show almost no heating rate dependence, which agrees well with that of PLLA crystallized at 80 °C reported by Kawai et al. [16], indicating that the transformation from the α' crystalline phase to α one is a solid state transition. This is a further clue that the multiple melting behavior of samples crystallized in Region I arises from the polymorphous transition rather than melt–recrystallization.

Effect of crystallization time

To explore the influence of crystallization time (t_c) on the melting behavior of PLLA, the DSC heating scans of samples melt-crystallized at 90 °C for various times (from 10 to 240 min) were recorded and shown in Fig. 6. It is found that the samples cannot finish the crystallization within 60 min at 90 °C due to the slow crystallization rate of PLLA, and a broad cold-crystallization peak (T_{cc}) appears at 100–140 °C in the subsequent heating process. As expected, the longer the crystallization time is, the weaker the cold-crystallization peak. It is interesting that an additional endothermic peak (T_{cm}) presents between the low-temperature (T_{m1}) and high-temperature (T_{m1}) melting peaks, which can be assigned to the melting of crystals generated in the cold-crystallization process. When t_c is longer than 60 min, the endothermic peak (T_{cm}) disappears due to the completion of isothermal melt-crystallization. The amount of crystallites formed in the isothermal crystallization increases with t_c , and they may serve as

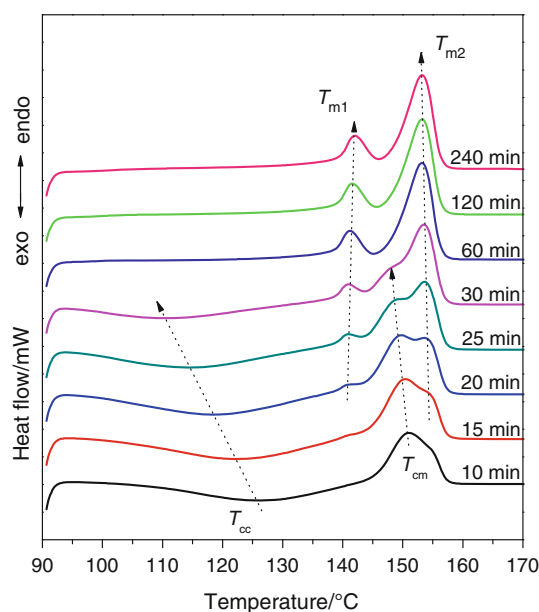


Fig. 6 DSC heating scans obtained at 10 °C min⁻¹ of PLLA melt-crystallized at 90 °C for different times as indicated

nucleating sites to promote the subsequent cold-crystallization; as a result, both T_{cc} and T_{cm} decrease with increasing t_c . Furthermore, lamella thickening usually occurs by prolonging the crystallization time leading to the peak I (T_{m1}) slightly shifts to a higher temperature with t_c as can be seen in Fig. 6.

Conclusions

Effects of crystallization temperature, time, and heating rate on the melting behavior of PLLA with a low optical purity of 92 % were studied by DSC in detail. In these PLLA samples, the disordered (α') and ordered (α) crystals are mainly formed at $T_c < 95$ °C and $T_c \geq 95$ °C, respectively. The melting behavior of PLLA is strongly dependent on T_c and is distinct in three temperature regions: Region I ($T_c < 95$ °C), Region II (95 °C $\leq T_c < 120$ °C), and Region III ($T_c \geq 120$ °C), in which triple (including two endotherms and one exotherm), double, and single endothermic peaks were observed, respectively. The multiple melting behavior of the PLLA samples crystallized at lower temperatures (Region I) can be attributed to the direct melting of partial α' crystals, α' -to- α crystalline phase transition, and the melting of the as-transformed α crystals. Similar to the non-polymorphous polymers, the melting of samples crystallized at higher temperatures is in the melt-recrystallization mechanism (Region II) or by the direct melting of the perfect α crystals (Region III). The influence of crystallization time on the melting behavior of PLLA shows that the prolonged time makes the low-temperature endothermic peak shift slightly to a higher temperature.

Acknowledgements The work was financially supported by the National Natural Science Foundation of China (No. 30870633, 31000427) and the Fundamental Research Funds for the Central Universities (No. DUT12JB09).

References

1. Drumright RE, Gruber PR, Henton DE. Polylactic acid technology. *Adv Mater.* 2000;12:1841–6.
2. Pan P, Inoue Y. Polymorphism and isomorphism in biodegradable polyesters. *Prog Polym Sci.* 2009;34:605–40.
3. Rasal RM, Janorkar AV, Hirt DE. Poly(lactic acid) modifications. *Prog Polym Sci.* 2010;35:338–56.
4. De Santis P, Kovacs AJ. Molecular conformation of poly(S-lactic acid). *Biopolymers.* 1968;6:299–306.
5. Miyata T, Masuko T. Morphology of poly(L-lactide) solution-grown crystals. *Polymer.* 1997;38:4003–9.
6. Alemán C, Lotz B, Puiggali J. Crystal structure of the α -form of poly(L-lactide). *Macromolecules.* 2001;34:4795–801.
7. Sasaki S, Asakura T. Helix distortion and crystal structure of the α form of poly(L-lactide). *Macromolecules.* 2003;36:8385–90.
8. Eling B, Gogolewski S, Pennings AJ. Biodegradable materials of poly(L-lactic acid): 1. Melt-spun and solution-spun fibres. *Polymer.* 1982;23:1587–93.
9. Hoogsteen W, Postema AR, Pennings AJ, Ten Brinke G, Zugenmaier P. Crystal structure, conformation, and morphology of solution-spun poly(L-lactide) fibers. *Macromolecules.* 1990;23:634–42.
10. Puiggali J, Ikada Y, Tsuji H, Cartier L, Okihara T, Lotz B. The frustrated structure of poly(L-lactide). *Polymer.* 2000;41:8921–30.
11. Cartier L, Okihara T, Ikada Y, Tsuji H, Puiggali J, Lotz B. Epitaxial crystallization and crystalline polymorphism of poly-lactides. *Polymer.* 2000;41:8909–19.
12. Zhang J, Duan Y, Sato H, Tsuji H, Noda I, Yan S, Ozaki Y. Crystal modifications and thermal behavior of poly(L-lactic acid) revealed by infrared spectroscopy. *Macromolecules.* 2005;38:8012–21.
13. Zhang J, Tashiro K, Domb AJ, Tsuji H. Confirmation of disorder α form of poly(L-lactic acid) by the X-ray fiber pattern and polarized IR/Raman spectra measured for uniaxially-oriented samples. *Macromol Symp.* 2006;242:274–8.
14. Pan P, Kai W, Zhu B, Dong T, Inoue Y. Polymorphous crystallization and multiple melting behavior of poly(L-lactide): molecular weight dependence. *Macromolecules.* 2007;40:6898–905.
15. Pan P, Zhu B, Kai W, Dong T, Inoue Y. Effect of crystallization temperature on crystal modifications and crystallization kinetics of poly(L-lactide). *J Appl Polym Sci.* 2008;107:54–62.
16. Kawai T, Rahman N, Matsuba G, Nishida K, Kanaya T, Nakano M, Okamoto H, Kawada J, Usuki A, Honma N, Nakajima K, Matsuda M. Crystallization and melting behavior of poly(L-lactic acid). *Macromolecules.* 2007;40:9463–9.
17. Salmerón Sánchez M, Mathot VBF, Vanden Poel G, Gómez Ribelles JL. Effect of the cooling rate on the nucleation kinetics of poly(L-lactic acid) and its influence on morphology. *Macromolecules.* 2007;40:7989–97.
18. Cho TY, Strobl G. Temperature dependent variations in the lamellar structure of poly(L-lactide). *Polymer.* 2006;47:1036–43.
19. Pantani R, De Santis F, Sorrentino A, De Maio F, Titomanlio G. Crystallization kinetics of virgin and processed poly(lactic acid). *Polym Degrad Stab.* 2010;95:1148–59.
20. Di Lorenzo ML. Crystallization behavior of poly(L-lactic acid). *Eur Polym J.* 2005;41:569–75.
21. Di Lorenzo ML. The crystallization and melting processes of poly(L-lactic acid). *Macromol Symp.* 2006;234:176–83.
22. Yasuniwa M, Tsubakihara S, Iura K, Ono Y, Dan Y, Takahashi K. Crystallization behavior of poly(L-lactic acid). *Polymer.* 2006;47:7554–63.
23. Krache R, Benavente R, López Majada JM, Perena JM, Cerrada ML, Pérez E. Competition between α , β , and γ polymorphs in a β -nucleated metallocenic isotactic polypropylene. *Macromolecules.* 2007;40:6871–8.
24. De Rosa C, Auremma F, Vinti V, Galimberti M. Equilibrium melting temperature of syndiotactic polypropylene. *Macromolecules.* 1998;31:6206–10.
25. Liu T, Petermann J. Multiple melting behavior in isothermally cold-crystallized isotactic polystyrene. *Polymer.* 2001;42:6453–61.
26. Lee Y, Porter RS. Double-melting behavior of poly(ether ether ketone). *Macromolecules.* 1987;20:1336–41.
27. Lee Y, Porter RS, Lin JS. On the double-melting behavior of poly(ether ether ketone). *Macromolecules.* 1989;22:1756–60.
28. Lattimer MP, Hobbs JK, Hill MJ, Barham PJ. On the origin of the multiple endotherms in PEEK. *Polymer.* 1992;33:3971–3.
29. Wang ZG, Hsiao BS, Sauer BB, Kampert WG. The nature of secondary crystallization in poly(ethylene terephthalate). *Polymer.* 1999;40:4615–27.

30. Kong Y, Hay JN. Multiple melting behaviour of poly(ethylene terephthalate). *Polymer*. 2003;44:623–33.
31. Ju MY, Chang FC. Multiple melting behavior of poly(butylene-2,6-naphthalate). *Polymer*. 2001;42:5037–45.
32. Srimoan P, Dangseeun N, Supaphol P. Multiple melting behavior in isothermally crystallized poly(trimethylene terephthalate). *Eur Polym J*. 2004;40:599–608.
33. Yasuniwa M, Satou T. Multiple melting behavior of poly(butylene succinate). I. Thermal analysis of melt-crystallized samples. *J Polym Sci Part B Polym Phys*. 2002;40:2411–20.
34. Xu Y, Xu J, Guo B, Xie X. Crystallization kinetics and morphology of biodegradable poly(butylene succinate-co-propylene succinate)s. *J Polym Sci Part B Polym Phys*. 2007;45:420–8.
35. Wang Y, Bhattacharya M, Mano JF. Thermal analysis of the multiple melting behavior of poly(butylene succinate-co-adipate). *J Polym Sci Part B Polym Phys*. 2005;43:3077–82.
36. Gunaratne LMWK, Shanks RA. Multiple melting behaviour of poly(3-hydroxybutyrate-co-hydroxyvalerate) using step-scan DSC. *Eur Polym J*. 2005;41:2980–8.
37. Shan GF, Yang W, Tang XG, Yang MB, Xie BH, Fu Q, Mai YW. Multiple melting behavior of annealed crystalline polymers. *Polym Test*. 2010;29:273–80.
38. Yasuniwa M, Tsubakihara S, Sugimoto Y, Nakafuku C. Thermal analysis of the double-melting behavior of poly(L-lactic acid). *J Polym Sci Part B Polym Phys*. 2004;42:25–32.
39. Di Lorenzo ML. Calorimetric analysis of the multiple melting behavior of poly(L-lactic acid). *J Appl Polym Sci*. 2006;100:3145–51.
40. Ling X, Spruiell JE. Analysis of the complex thermal behavior of poly(L-lactic acid) film. I. Samples crystallized from the glassy state. *J Polym Sci Part B Polym Phys*. 2006;44:3200–14.
41. Ling X, Spruiell JE. Analysis of the complex thermal behavior of poly(L-lactic acid) film. II. Samples crystallized from the melt. *J Polym Sci Part B Polym Phys*. 2006;44:3378–91.
42. Shieh YT, Liu GL. Temperature-modulated differential scanning calorimetry studies on the origin of double melting peaks in isothermally melt-crystallized poly(L-lactic acid). *J Polym Sci Part B Polym Phys*. 2007;45:466–74.
43. Yasuniwa M, Iura K, Dan Y. Melting behavior of poly(L-lactic acid): effects of crystallization temperature and time. *Polymer*. 2007;48:5398–407.
44. Wang Y, Mano JF. Role of thermal history on the thermal behavior of poly(L-lactic acid) studied by DSC and optical microscopy. *J Therm Anal Calorim*. 2005;80:171–5.
45. Yasuniwa M, Sakamo K, Ono Y, Kawahara W. Melting behavior of poly(L-lactic acid): X-ray and DSC analyses of the melting process. *Polymer*. 2008;49:1943–51.
46. Su Z, Li Q, Liu Y, Hu GH, Wu C. Multiple melting behavior of poly(lactic acid) filled with modified carbon black. *J Polym Sci Part B Polym Phys*. 2009;47:1971–80.
47. Xu HS, Dai XJ, Lamb PR, Li ZM. Poly(L-lactide) crystallization induced by multiwall carbon nanotubes at very low loading. *J Polym Sci Part B Polym Phys*. 2009;47:2341–52.
48. Calafe M, Remiro PM, Cortázar MM, Calahorra ME. Cold crystallization and multiple melting behavior of poly(L-lactide) in homogeneous and in multiphase epoxy blends. *Colloid Polym Sci*. 2010;288:283–96.
49. Shen C, Wang Y, Li M, Hu D. Crystal modifications and multiple melting behavior of poly(L-lactic acid-co-D-lactic acid). *J Polym Sci Part B Polym Phys*. 2011;49:409–13.
50. Lan Q, Yu J, He J, Maurer FHJ, Zhang J. Thermal behavior of poly(L-lactide) having low L-isomer content of 94 % after compressed CO₂ treatment. *Macromolecules*. 2010;43:8602–9.
51. Sarasua JR, Prud'homme RE, Wisniewski M, Borgne AL, Spassky N. Crystallization and melting behavior of poly(lactides). *Macromolecules*. 1998;31:3895–905.
52. Kolstad JJ. Crystallization kinetics of poly(L-lactide-co-meso-lactide). *J Appl Polym Sci*. 1996;62:1079–91.
53. Huang J, Lisowski MS, Runt J, Hall ES, Kean RT, Buehler N, Lin JS. Crystallization and microstructure of poly(L-lactide-co-meso-lactide) copolymers. *Macromolecules*. 1998;31:2593–9.
54. Tsuji H, Ikada Y. Crystallization from the melt of poly(lactide)s with different optical purities and their blends. *Macromol Chem Phys*. 1996;197:3483–99.
55. Di Lorenzo ML, Cocca M, Malinconico M. Crystal polymorphism of poly(L-lactic acid) and its influence on thermal properties. *Thermochim Acta*. 2011;522:110–7.
56. Cocca M, Di Lorenzo ML, Malinconico M, Frezza V. Influence of crystal polymorphism on mechanical and barrier properties of poly(L-lactic acid). *Eur Polym J*. 2011;47:1073–80.
57. Zhang J, Tashiro K, Tsuji H, Domb AJ. Disorder-to-order phase transition and multiple melting behavior of poly(L-lactide) investigated by simultaneous measurements of WAXD and DSC. *Macromolecules*. 2008;41:1352–7.
58. Baratian S, Hall ES, Lin JS, Xu R, Runt J. Crystallization and solid-state structure of random polylactide copolymers: poly(L-lactide-co-D-lactide)s. *Macromolecules*. 2001;34:4857–64.
59. Abe H, Harigaya M, Kikkawa Y, Tsuge T, Doi Y. Crystal growth and solid-state structure of poly(lactide) stereocopolymers. *Biomacromolecules*. 2005;6:457–67.
60. Pan P, Liang Z, Zhu B, Dong T, Inoue Y. Blending effects on polymorphic crystallization of poly(L-lactide). *Macromolecules*. 2009;42:3374–80.
61. Pan P, Zhu B, Kai W, Dong T, Inoue Y. Polymorphic transition in disordered poly(L-lactide) crystals induced by annealing at elevated temperatures. *Macromolecules*. 2008;41:4296–304.
62. Hoffman JD, Weeks JJ. Melting process and the equilibrium melting temperature of polychlorotrifluoroethylene. *J Res Natl Bur Stand Sect A*. 1962;66:13–28.